FAST SUBJECT SPECIFIC FINITE ELEMENT MESH GENERATION OF KNEE JOINT FROM BIPLANAR X-RAY IMAGES

Bhrigu K. Lahkar[*], Pierre-Yves Rohan[*], Helene Pillet[*], Patricia Thoreux[*, †], Wafa Skalli[*]

[*] Institut de Biomécanique Humaine Georges Charpak,
Arts et Métiers ParisTech, Paris, France
brighu_kumar.lahkar@ensam.eu

[†]Université Paris 13
Sorbonne Paris Cité, Bobigny, France
patricia.thoreux@aphp.fr

Keywords: FEM, 3D reconstruction, subject specific mesh, knee joint, biplanar X-ray.

Abstract: *An accurate and fast computational mesh generation is a prerequisite to perform personalized FE analyses. Traditionally, both triangular/tetrahedral and quadrilateral/hexahedral FE elements are used for 3D mesh generation. But because of distinct numerical advantages, hexahedral elements are preferred to avoid numerical instability. Here, we propose a methodology to develop fast and automatic subject specific mesh for knee joint from biplanar X-ray images. This methodology first involves building 3D reconstruction from biplanar radiographic image and then generating generic linear hexahedral mesh for the femur, tibia and patella. The generic mesh (GM) for individual bony structure is then deformed to obtain subject specific mesh (SSM) based on kriging interpolation. Meshing of both the meniscus follows a different approach where the surface nodes of the femur and tibia are used to generate linear hexahedral elements mesh. This complete methodology was successfully tested on 11 cadaveric specimens with approximately 12 min computational time for each out of which 3D reconstruction time was nearly 10 min. Numerical cost involved in deforming mesh for each specimen was 30 sec and generating mesh for both the meniscus was nearly 1 min. Mesh quality was assessed using standard ANSYS mesh quality indicators (aspect ratio, parallel deviation, maximum angle, Jacobian ratio and warping factor). For each specimen the value of total warnings above threshold showed in the range of 0.38−0.59% with no error. Surface mesh accuracy was evaluated as the point-to-surface distance between 3D reconstruction and subject specific mesh and the mean RMS values were reported. For all specimens, mean (RMS) errors in mm were respectively less than or equal to 0.2 (0.3), 0.3 (0.55) and 0.0 (0.1) for femur, tibia and patella which are less than the uncertainties of 3D reconstruction.*

Bhrigu K. Lahkar, Pierre-Yves Rohan, Helene Pillet, Patricia Thoreux, Wafa Skalli

1 INTRODUCTION

Numerous finite element models of the knee joint have been developed to investigate knee injury mechanism [1], surgery assessment [2, 3] and contact kinematics at knee joint [4−6]. However, because of extensive computational effort required for preparing subject specific model from CT-scan or MRI data, most of the models in literature are done only for one or very few subjects. This results in poor validation of the model while dealing with patient specific estimation of tissue response as well as studying effect of morphological inter-subject variability. As an alternative to CT scan and MRI data, use of biplanar X-ray image is promising to perform 3D reconstructions of bony structures [7−9] because of low radiation dose, very little reconstruction time and ability to replicate complex bony structure with ease.

The quality of FE mesh plays vital role in obtaining reliable and accurate results. Traditionally, tetrahedral meshes are easy to generate but it reduces order of convergence for strains and stresses [10] and suffers numerical stability issues associated to shear locking and volumetric locking [11, 12]. Moreover, a FE mesh with tetrahedral elements require more elements as compared to hexahedral elements to achieve same solution accuracy leading to higher computational cost [13]. To avoid these issues, hexahedral elements are preferred for designing biomedical models [14, 15].

Building automatic FE mesh with hexahedral elements is time consuming and restrictive [16]. Literature shows majority of articles deal with fast and robust automatic methods to generate tetrahedral mesh of arbitrary geometries [17, 18]. Though, very few teams reported on automatic generation of hexahedral meshes using different techniques, the use of automatic hexahedral mesh generation is still limited due to robustness issues [15].

The objective of the present study was motivated by previous successful implementation of subject specific FE modelling on lower cervical spine [19]. Here, a specific approach to automatically generate subject specific FE mesh from biplanar X-ray images is proposed for knee joint structure.

2 MATERIALS AND METHOD

Eleven healthy lower limb cadaveric specimens aged between 47 and 79 years were used in this work based upon a previous study [20]. Each specimen includes femur, tibia and patella with joint passive structures intact.

The overall methodology of the current study uses following steps: (a) acquisition of biplanar radiographic image for specimens of interest, (b) 3D reconstruction of femur, tibia and patella, (c) generation of GM of whole knee joint, (d) deformation of GM to obtain SSM, (e) mesh quality evaluation of SSM and (f) surface representation accuracy computation. The work flow of this approach is represented in Fig.1 and is restricted to the mesh generation of the bony structures only. A different methodology is followed to generate mesh for meniscus.
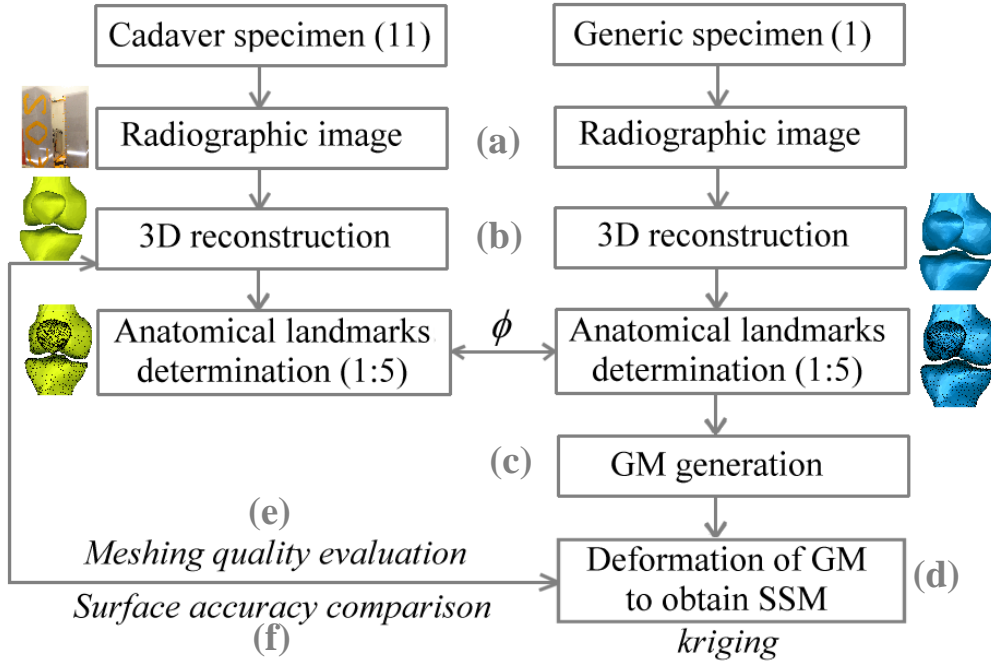
Figure 1: Overall workflow of subject specific mesh generation for bony structures. The process follows (a) acquisition of radiographic image for knee specimens, (b) 3D reconstruction of bony structures and anatomical landmark determination for each, (d) generation of generic mesh (GM), (d) GM deformation to obtain subject specific mesh (SSM) by numerical interpolation, (e) mesh quality evaluation of the SSM and (f) surface accuracy comparison between the SSM and 3D reconstruction.

2.1 Mesh generation of bony structures

First, biplanar radiographic images of bony structures (femur, tibia and patella) for one of the cadaveric specimens (named as generic) as well as all the 11 specimens of interest were acquired using EOS low dose imaging device (EOS®, EOS-imaging, France). Then from the radiographic images, 3D digital models of all specimens were obtained using 3D reconstruction algorithm validated by previous studies with reconstruction time of 10 min for each specimen [9, 21, 22]. As a reminder, 3D reconstruction process begins with identification and labelling of various anatomical regions and landmarks on the biplanar images. Next, based on statistical inferences a simplified personalized parametric model (SPPM) is generated. After that, the morpho-realistic 3D generic model is deformed towards the SPPM to obtain morpho-realistic personalized parametric model (MPPM) using moving least square and kriging interpolation [23]. Finally, this MPPM is manually adjusted till the best estimate of the respective subject specific model (Fig. 2).
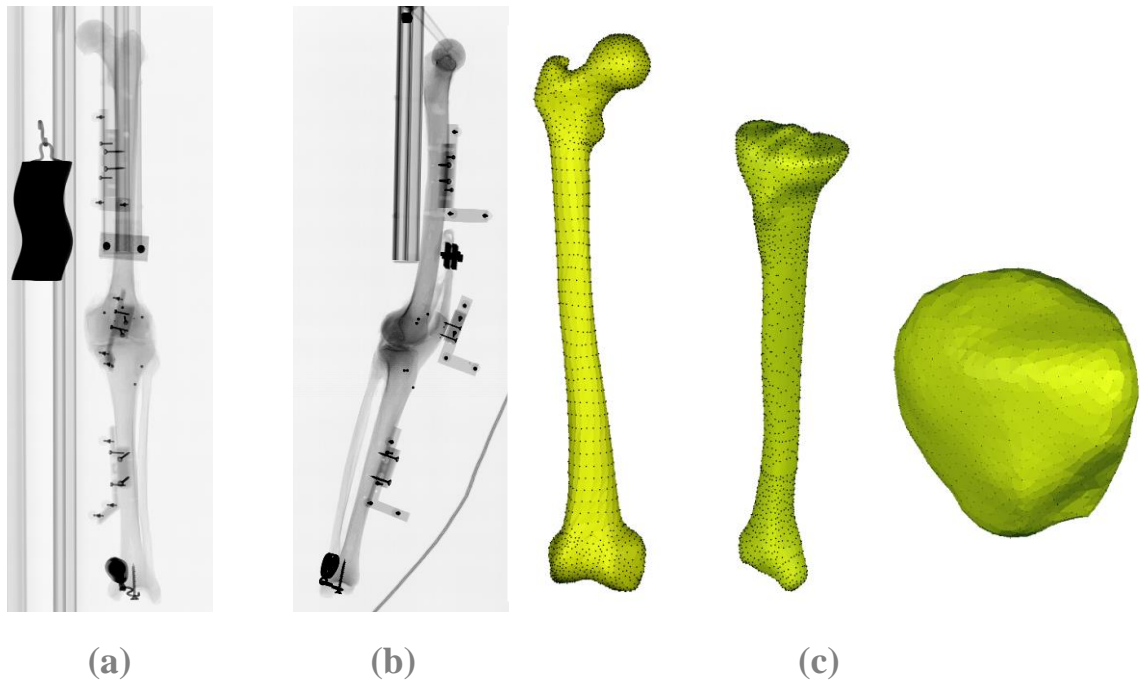
(a) **(b)** **(c)**

Figure 2: An example of radiograph in (a) frontal, (b) sagittal view and its (c) 3D reconstruction model of femur, tibia and patella

In the following step, the generic 3D reconstruction was imported into Geomagic Studio 12.0 (3D systems, Carolina, USA) for manual patch construction so as to form sets of deformed cubes in the model. Then the CAD model was imported to a customized Matlab (Mathworks, Massachusetts, United States) routine to create volumetric mesh. Here, each deformed cube was discretized into sets of small blocks. This was done by discretizing the edges of the deformed cube, then the faces followed by the whole cube. Thus, generic linear hexahedral mesh was generated for 1 deformed cube first and then for the remaining with the same process. Fig. 3 shows generic FE meshed model development process for femur. Similar approach was implemented for generic tibia and patella.
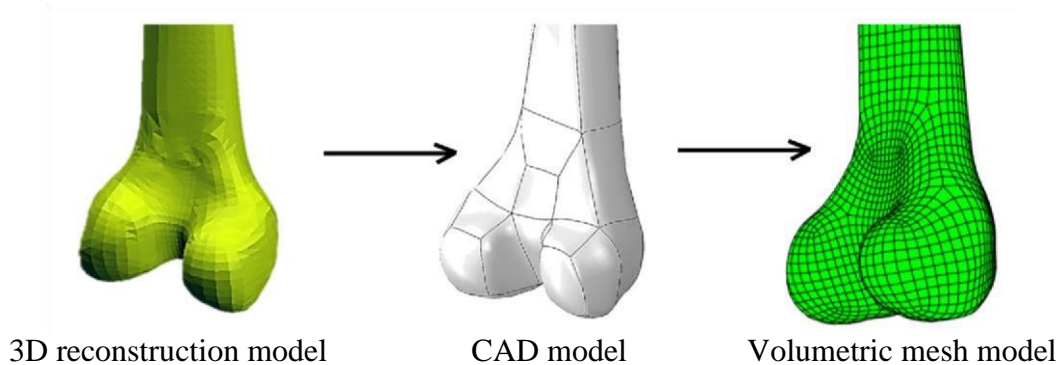

3D reconstruction model   CAD model   Volumetric mesh model

Figure 3: Generic meshed model development sequence for femur (only distal epiphysis is shown for clarity)

Finally, a mapping (φ, as drift and fluctuation) from source (generic) to target (subject specific) points was evaluated by applying dual kriging interpolation [23]. Then, on the basis of the mapping, the generic mesh (GM) of individual specimen was deformed to obtain subject specific mesh (SSM) using numerical interpolation. Mesh deformation was done in a customized Matlab routine with computational cost nearly 30 sec for each specimen.

2.2 Mesh generation of meniscus

At first, 2 splines were constructed through the selected nodes of the surface meshes of medial tibial plateau (Fig. 4(a)). Then, the nodes on tibial splines were used for searching nearest nodes on the medial femoral condyle using nearest-neighbor interpolation. Another, 2 splines were constructed through these searched nodes on femoral condyle. These splines were then connected with straight lines at the extreme nodes. Finally, these splines and the lines were discretized into respectively 50, 5 and 4 no of divisions circumferentially (c), radially (r) and axially (a) (Fig. 4(b)). Then by establishing element connection volumetric mesh (linear hexahedral) was created for the meniscus (Fig. 4(c)). Similar procedure was followed to generate mesh for the lateral meniscus with numerical cost less than 1 min in a custom made Matlab routine.

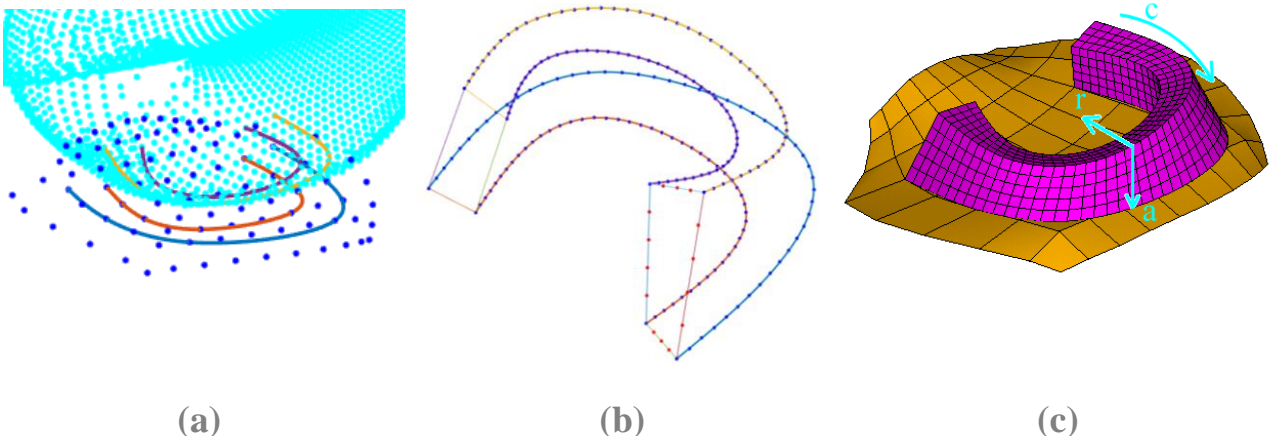<div align="center">(a)   (b)   (c)</div>

Figure 4: Mesh generation process of meniscus (a) Spline construction through the surface nodes of femoral condyle and tibial plateau, (b) discretization of splines & connecting lines and (c) volumetric meshed generation (shown for only medial meniscus).

2.3 Mesh quality evaluation

Mesh quality was assessed using standard ANSYS mesh quality indicators: aspect ratio, parallel deviation, maximum angle, Jacobian ratio and warping factor. The default warning (error) threshold values for linear hex elements are 20(1000000), 70(150), 155(179.9), 30(1000) and 0.2(0.4) respectively.

2.4 Surface representation accuracy

The accuracy of subject specific mesh for each specimen was compared against respective 3D reconstruction model by registering point-to-surface distance. This was done in a custom made Matlab routine by projecting the subject specific mesh on the 3D model and the error computed (mean, RMS) was also visualized.

3 RESULTS AND DISCUSSION

With the fully automated methodology described, subject specific mesh for all 11 knee joint specimens were generated. Fig. 5 illustrates all the generated meshes using this methodology.
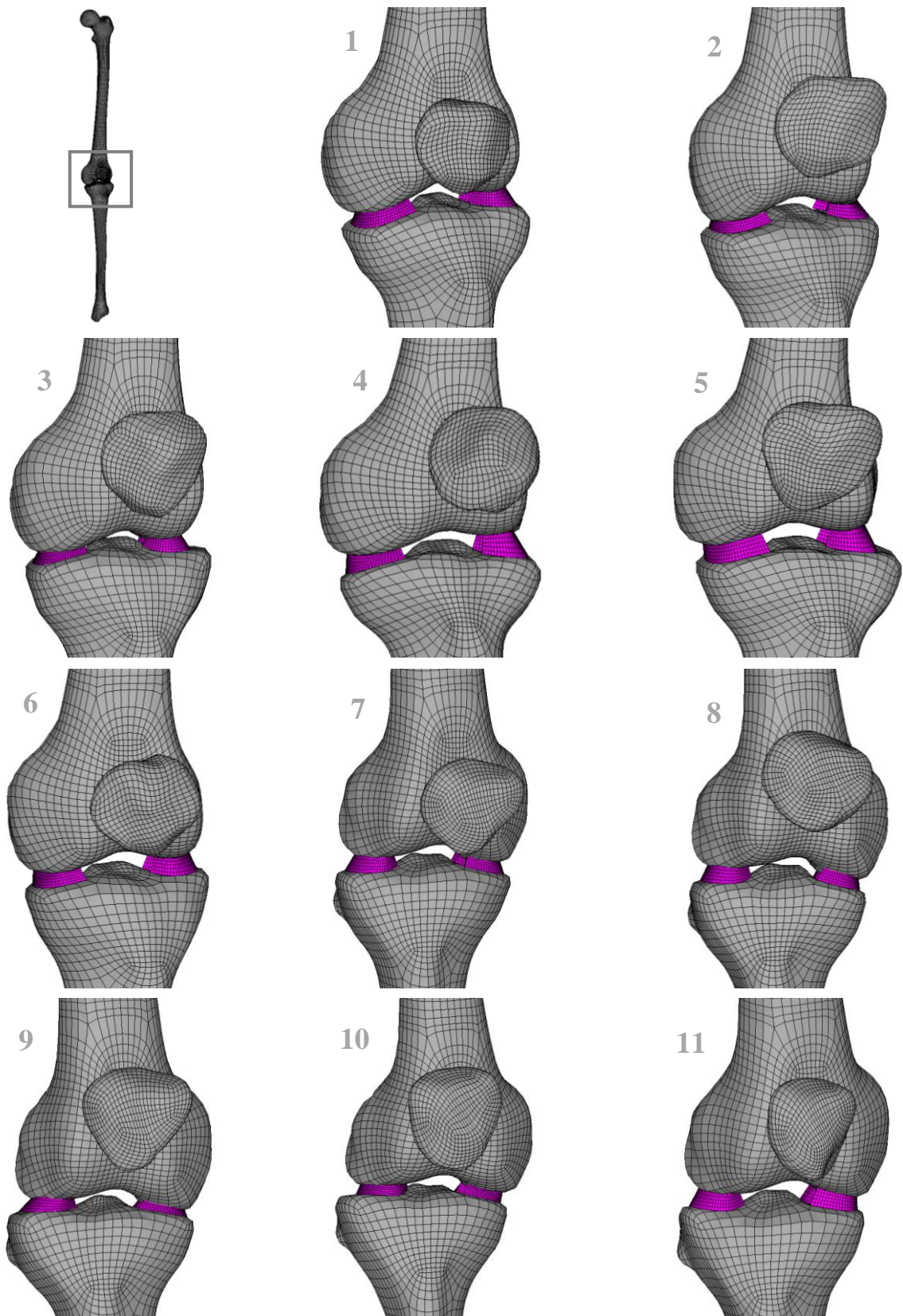
Figure 5: Global mesh of knee joint for all the 11 specimens. For clarity only the distal epiphysis of femur and proximal epiphysis of tibia is shown.

3.1 Mesh quality

Quality of individual knee joint mesh is represented in Table 1 in terms of mesh quality indicators (warning % above threshold value). Maximum warnings can be seen in the case of maximum angle followed by aspect ratio. There are no occurrence of errors in any mesh and total warning percentage is satisfactorily very less with a maximum value of 0.59% for specimen 10.

FE model	Aspect ratio	Parallel deviation	Maximum angle	Jacobian ratio	Warping factor
Specimen 1	0.12	0.03	0.25	0.01	0.04
Specimen 2	0.20	0.03	0.16	0.01	0.05
Specimen 3	0.16	0.03	0.21	0.01	0.04
Specimen 4	0.14	0.03	0.36	0.01	0.04
Specimen 5	0.18	0.03	0.21	0.01	0.04
Specimen 6	0.12	0.04	0.17	0.01	0.04
Specimen 7	0.13	0.05	0.22	0.01	0.04
Specimen 8	0.21	0.02	0.25	0.01	0.04
Specimen 9	0.16	0.03	0.25	0.01	0.04
Specimen 10	0.20	0.04	0.30	0.01	0.04
Specimen 11	0.12	0.04	0.23	0.01	0.04

Table 1: Mesh quality of each specimen in terms of warning percentage above threshold. Here the warning percentage in each indicator signifies the no of warning counts above thershold divided by total no of elements in percentage.

3.2 Surface representation accuracy

Table 2 represents surface accuracy of individual specimen. For femur and tibia mean (RMS) error in mm varies in the range of 0.1–0.2 (0.2–0.3) and 0.2–0.3 (0.4–0.55) respectively, whereas in the case of patella no mean error can be seen with RMS error varying in the range 0.05–0.1. Overall, subject specific mesh of patella showed highest closeness to the 3D reconstruction model followed by femur and tibia.

Specimen	Mean (RMS) error in mm		
	Femur	Tibia	Patella
Specimen 1	0.2 (0.30)	0.3 (0.50)	0 (0.10)
Specimen 2	0.1 (0.25)	0.2 (0.50)	0 (0.10)
Specimen 3	0.1 (0.25)	0.3 (0.50)	0 (0.10)
Specimen 4	0.1 (0.20)	0.2 (0.40)	0 (0.05)
Specimen 5	0.1 (0.20)	0.2 (0.45)	0 (0.05)
Specimen 6	0.1 (0.25)	0.3 (0.50)	0 (0.10)
Specimen 7	0.1 (0.25)	0.3 (0.50)	0 (0.00)
Specimen 8	0.1 (0.25)	0.2 (0.50)	0 (0.05)
Specimen 9	0.1 (0.25)	0.3 (0.55)	0 (0.05)
Specimen 10	0.1 (0.25)	0.2 (0.40)	0 (0.05)
Specimen 11	0.1 (0.25)	0.3 (0.50)	0 (0.10)

Table 2: Surface representation accuracy of individual specimen.

Suface representation accuracy for the entire geomtery of femur, tibia and patella of each specimen were visualized and as an example illustrated in Fig. 6 for specimen 1.

Close-up view in the functional region of knee joint are shown for femur and tibia.
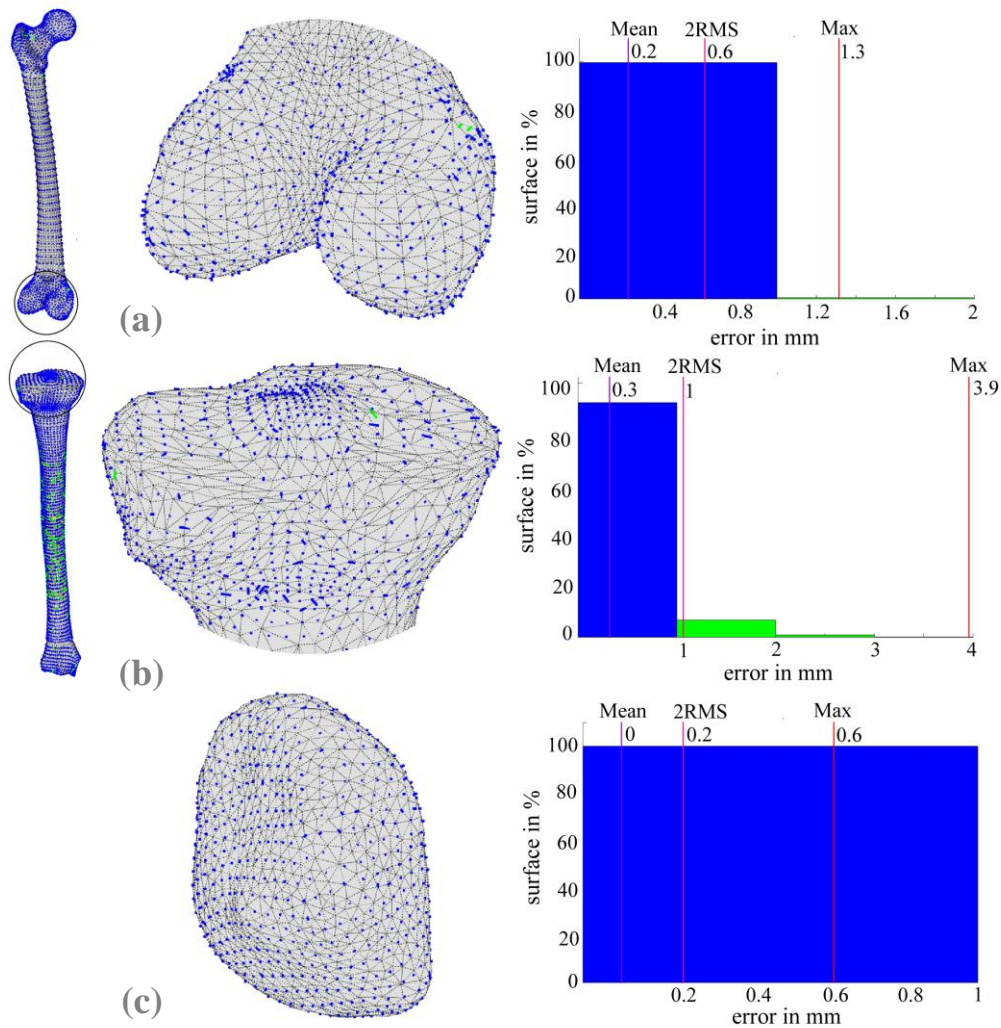

Figure 6: Surface representation accuracy as point-to-surface distance for (a) femur, (b) tibia and (c) patella

4   CONCLUSIONS

The scientific issue addressed in this study is one of the prevailing challenges faced by the researchers and clinicians to account for inter-subject variability in their investigations. While referring to morphological variations between subjects, the key technical hurdles often arise are the automatic generation of hexahedral mesh for individuals with minimum possible time and without compromising mesh quality. Majority of the existing methods requires substantial amount of time to generate patient specific hexahedral mesh for individual geometry. This is mainly due to the time involved in manual segmentation of images acquired from CT or MRI data.

Our methodology proposed in the current study mainly relies on careful design of a generic FE mesh from 3D reconstruction of the target structure with proper anatomical features of interest. Proper caution requires in the functional areas: contact surface and ligament insertion sites of the knee joint. This preliminary work is a one-time effort,

henceforth to establish automatic mesh deformation from generic to subject-specific.

In all the studied specimens, 3D reconstruction time was nearly 10 min for individuals which is in contrast to the approach with CT or MRI. In all the FE models the regularity of the subject specific mesh is preserved without excessive distortion. Mesh quality of individual mesh is very good with above threshold warning percentage in the range of 0.38−0.59%. Again, the algorithm employed in the current methodology was able to closely replicate the bony structures of individuals maintaining satisfactory surface representation accuracy.

To our best knowledge, no such methodology is developed till now especially for knee joint which can allow generation of nearly accurate mesh from 3D reconstruction for any no of specimens. Because of fastness and subject specificity in terms of geometry this methodology has the full potential to be implemented in clinical routine to investigate personalized characteristics of the knee, e.g. post-surgery treatment, impact of using medical devices and also inter individual variation of knee morphology on its biomechanics. This study also opens new perspective to develop hexahedral FE mesh for subjects in-vivo.

Acknowledgement

REFERENCES

[1] A. Kiapour, A.M. Kiapour, V. Kaul, C.E. Quatman, S.C. Wordeman, T.E. Hewett, C.K. Demetropoulos, V.K. Goel. Finite element model of the knee for investigation of injury mechanisms: development and validation. *Journal of Biomechanical Engineering*, 136(1), 0110021–01100214, 2014.

[2] K.T. Kang, Y.G. Koh, J. Son, O.R. Kwon, J.S. Lee, S.K. Kwon. A computational simulation study to determine the biomechanical influence of posterior condylar offset and tibial slope in cruciate retaining total knee arthroplasty. *Bone and Joint Research*, 31(01), 7(1), 69–78, 2018.

[3] X. Xie, R. Rusly, J.D DesJardins, F. Voss, K. Chillag, M. LaBerge. Effect of rotational prosthetic alignment variation on tibiofemoral contact pressure distribution and joint kinematics in total knee replacement. Proceedings of the Institution of Mechanical Engineers, Part H: *Journal of Engineering in Medicine*, 231(11), 1034–1037, 2017.

[4] T.L. Donahue, M.L. Hull, M.M. Rashid, C.R. Jacobs. A finite element model of the human knee joint for the study of tibio-femoral contact. *Journal of Biomechanical Engineering*, 124(3), 273–80, 2002.

[5] S. Koo, J.H. Rylander, T.P. Andriacchi. Knee Joint Kinematics during Walking Influences the Spatial Cartilage Thickness Distribution in the Knee. *Journal of Biomechanics*, 44(7), 1405–1409, 2012.

[6] A. Ali, S. Shalhoub, A. Cyr, C. Fitzpatrick, L. Maletsky, P. Rullkoetter, K. Shelburne. Validation of predicted patellofemoral mechanics in a finite element model of the healthy and cruciate-deficient knee. *Journal of Biomechanics*, 49(2), 302–309, 2016.

[7] T. Sato, Y. Koga, G. Omori. Three-dimensional lower extremity alignment assessment system: application to evaluation of component position after total knee arthroplasty. *Journal of Arthroplasty*, 19(5), 620–628, 2004.

[8] M.K. Lee, S.H. Lee, A. Kim, I. Youn, T.S. Lee, N. Hur, K. Choi. The study of femoral 3D reconstruction process based on anatomical parameters using a numerical method. *Journal of Biomechanical Science and Engineering*, 3(3), 443–451, 2008.

[9]   Y. Chaibi , T. Cresson , B. Aubert , J. Hausselle , P. Neyret , O. Hauger , J.A. de Guise, W. Skalli. Fast 3D reconstruction of the lower limb using a parametric model and statistical inferences and clinical measurements calculation from biplanar X-rays. *Computer Methods in Biomechanics and Biomedical Engineering*, 15(5), 457–466, 2011.

[10]   D.J. Payen, K.J. Bathe. Improved stresses for the 4-node tetrahedral element. *Computers & Structures*, 89(13–14), 1265–1273, 2011.

[11]   G.R. Joldes, A. Wittek, K. Mille. Non-locking tetrahedral finite element for surgical simulation. *Communications in Numerical Methods in Engineering*, 25: 827–836, 2009.

[12]   Y. Onishi, K. Amaya. A locking-free selective smoothed finite element method using tetrahedral and triangular elements with adaptive mesh rezoning for large deformation problems. *Numerical Methods in Engineering*, 99(5), 354–371, 2014.

[13]   A. Ramos, J.A. Simões. Tetrahedral versus hexahedral finite elements in numerical modelling of the proximal femur. *Medical Engineering & Physics*, 28(9), 916–924, 2006.

[14]   J.M. Gérard, R. W.-Tricarico, P. Perrier, Y. Payan. A 3D dynamical biomechanical tongue model to study speech motor control. *Recent Research Developments in Biomechanics,* 1, 49–64, 2003.

[15]   P.-Y. Rohan, C. Lobos, M. A. Nazari, P. Perrier, Y. Payan. Finite element models of the human tongue: a mixed-element mesh approach. *Computer Methods in Biomechanics and Biomedical Engineering*: *Imaging & Visualization*, 43(2), 390–400, 2016.

[16]   T.J. Tautges, T. Blacker, S.A. Mitchell. The whisker weaving algorithm: a connectivity-based method for constructing all-hexahedral finite element meshes. *International Journal for Numerical Methods in Engineering*, 39(19), 3327−3349, 1996.

[17]   R. Löhner, P. Parikh. Generation of three-dimensional unstructured grids by the advancing-front method. *International Journal for Numerical Methods in Fluids*, 8, 1135–1149, 1988.

[18]   M.A. Yerry, M.S. Shephard. Automatic three-dimensional mesh generation by the modified-octree technique. *International Journal for Numerical Methods in Fluids*, 20, 1965−1990, 1984.

[19]   A. Laville, S. Laporte, W. Skalli. Parametric and subject-specific finite element modelling of the lower cervical spine. Influence of geometrical parameters on the motion patterns. *Journal of Biomechanics*, 42(10), 1409−1415, 2009.

[20]   H. Pillet, E. Bergamini, G. Rochcongar, V. Camomilla, P. Thoreux, P. Rouch, A. Cappozzo, W. Skalli. Femur, tibia and fibula bone templates to estimate subject-specific knee ligament attachment site locations. *Journal of Biomechanics*, 49(14), 3523−3528, 2016.

[21]   S. Quijano, A. Serrurier, B. Aubert, S. Laporte, P. Thoreux, W. Skalli. Three-dimensional reconstruction of the lower limb from biplanar calibrated radiographs. *Medical Engineering & Physics*, 35(12), 1703–1712, 2013.

[22]   L. Dagneaux, P. Thoreux, B. Eustache, F. Canovas, W. Skalli. Sequential 3D analysis of patellofemoral kinematics from biplanar x-rays: In vitro validation protocol. *Orthopaedics & Traumatology: Surgery & Research*, 101(7), 811–818, 2015.

[23]   F. Trochu. A Contouring Program Based on Dual Kriging Interpolation. *Engineering with Computers*, 9(3), 160–177, 1993.